

# Zinc Oxide/Polypyrrole particle-decorated rod structure for NO<sub>2</sub> detection at low temperature

Vu Thanh Dong<sup>1</sup>, Pham Tien Hung<sup>2</sup>, Le Duc Anh<sup>1</sup>, Ly Quoc Vuong<sup>1</sup>,  
Dang Duy Khanh<sup>1</sup>, Nguyen Thi Huong<sup>1,\*</sup>

<sup>1</sup>*Institute of Chemistry and Materials, Academy of Military Science and Technology,  
17 Hoang Sam, Nghia Do, Cau Giay, Ha Noi, Viet Nam*

<sup>2</sup>*Department of Physics, Le Quy Don Technical University, 236 Hoang Quoc Viet, Co Nhue,  
Bac Tu Liem, Ha Noi, Viet Nam*

\*Emails: [nguyenhuong0916@gmail.com](mailto:nguyenhuong0916@gmail.com)

Received: 15 July 2023; Accepted for publication: 15 April 2024

**Abstract.** In this study, Zinc oxide (ZnO) nanoparticles with a size of about 50 - 70 nm were green-synthesized using tea leaves and ZnO/Polypyrrole (ZnO/PPy) nanocomposites were obtained by ultrasonic-assisted chemical polymerization method using pyrrole monomer and the nanoparticles. The characterization of the materials is conducted using several analytical techniques, including Field Emission Scanning Electron Microscopy (FESEM) and X-Ray Diffraction (XRD) and Ultraviolet visible spectrum (UV-Vis). The synthesized PPy material exhibits have a rod-shaped structure, diameter ranging from 100 to 200 nm. The ZnO/PPy nanocomposite system, consisting of PPy rods surrounded by ZnO particles. The gas sensing characteristics of the materials have also been investigated by measuring their sensitivity, response time, and stability to NO<sub>2</sub> at low temperature and different humidity. Notably, the material exhibits considerable sensitivity to NO<sub>2</sub> gas at low temperatures and the parameters related to response and recovery times are relatively rapid. Furthermore, a potential gas-sensing mechanism based on changes in the width of the depletion region is proposed.

**Keywords:** green synthesis, NO<sub>2</sub> gas sensor, ZnO, conductive polymer, low temperature.

**Classification numbers:** 2.4.2, 2.4.4, 2.9.4.

## 1. INTRODUCTION

Presently, the development of science and technology serving human life has become the fundamental issue of every country worldwide. The rapidly growing population and diverse life needs have led to an explosion of industries related to home appliances, vehicles, fossil fuels, and several others. Although this evolution helps human life to be significantly improved, innovative, and more comfortable, the by-products of emissions from these industries are also a terrible danger to the planet [1]. The fact that a series of diseases related to the central nervous system, brain, eyes, and lungs, such as bronchitis, headache, chest tightness, and vomiting, are the most typical instances of gas poisoning during tuberculosis [2]. Therefore, exploring toxic gas detection sensors has become one of the leading research directions of advanced materials

researchers with the aim of sustainable human development. Over the years, various sensing technologies, including electrochemical, optical fiber, and nanomaterials, have been applied. Most prominent among them are sensors based on metal oxide semiconductor (MOS) materials with simple synthesis processes and advantages such as low cost, portability, high sensitivity and selectivity without additional auxiliary equipment [3].

For chemo-resistive gas sensors based on MOS materials, Zinc Oxide (ZnO) is one of the potential materials due to its excellent physicochemical properties. ZnO has a wide band gap of 3.37 eV and possesses several benefits, such as biocompatibility, chemical stability, environmental sustainability, and cost-effectiveness in synthesis [4]. ZnO has a crystalline nature that enables the growth of diverse nanostructures, including nanoparticles, one-dimensional (1D), two-dimensional (2D), and three-dimensional (3D) structures [5]. Previous research has established that manipulating material morphology influences on the gas sensing capabilities of materials in the field of gas sensing research [6]. Nevertheless, the biggest obstacle of gas sensors based on ZnO material is the high operating temperature, which has a detrimental impact on the longevity and precision of ZnO-based sensors. With the objective of tackling this challenge, some methods, such as doped ZnO and ZnO heterostructures, have been investigated to enhance the sensor's sensitivity and selectivity while simultaneously reducing the operating temperature [7]. The combination of conductive polymers with ZnO, such as Polypyrrole (PPy), is regarded as one of the recent and effective methods among these advanced approaches [8]. The change of distribution and microstructural properties of Polypyrrole after incorporating ZnO in enhancing the sensing parameter of a gas sensor was proven. For instance, in 2020, Harpale et al. synthesized PPy-ZnO nanocomposite using electrochemical and SILAR methods. The nanocomposite sensor demonstrates enhanced NH<sub>3</sub> sensing characteristics in comparison to both the pristine ZnO sensor and other sensors. The significance of the PPy-ZnO nanocomposite sensor is underscored by the recorded sensor response of 82% at a temperature of 45°C and a concentration of 150 ppm NH<sub>3</sub> [9].

To the best of our knowledge, the investigation of ZnO/PPy-based gas sensors, especially the improvement of fabrication processes and gas selectivity enhancement, holds considerable promise for future development. Therefore, in the scope of this research, a green synthesis approach and chemical oxidation were employed to fabricate a ZnO/PPy nanocomposite material, followed by investigating the gas sensing characteristics of the sensor towards NO<sub>2</sub> gas. In particular, the ZnO nanoparticles were synthesized from green tea leaves and subsequently incorporated into the polymerization process involving Pyrrole monomers.

## 2. MATERIALS AND METHODS

### 2.1. Materials

Zinc acetate dihydrate ( $\text{Zn}(\text{CH}_3\text{COO})_2 \cdot 2\text{H}_2\text{O}$ ,  $\geq 98\%$ , Merck); Methyl Orange ( $\text{C}_{14}\text{H}_{14}\text{N}_3\text{NaO}_3\text{S}$ ,  $\geq 98\%$ , Macklin); Iron(III) chloride ( $\text{FeCl}_3$ ,  $\geq 97\%$ , Merck); Sodium hydroxide ( $\text{NaOH}$ ,  $\geq 98\%$ , Macklin); Ethanol ( $\text{C}_2\text{H}_6\text{O}$ ,  $\geq 95\%$ , Macklin), Pyrrole ( $\text{C}_4\text{H}_5\text{N}$ , 99%, Macklin), Ammonium hydroxide solution ( $\text{NH}_4\text{OH}$ , AR, 25 - 28%, Macklin), Deionized water ( $\text{H}_2\text{O}$ ).

Tea leaves (*Camellia Sinensis*) were procured from Tan Cuong Xanh Company Limited at 42 Tay Son Street, Dong Da District, Ha Noi, Viet Nam. All designated leaves for extraction are 5 - 7 cm long and 2.5 - 4 cm wide.

## 2.2. Methods

### 2.2.1. Extraction process

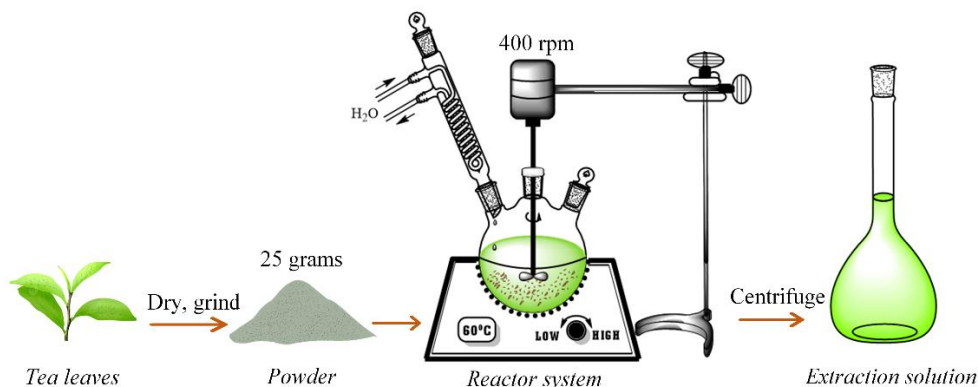


Figure 1. Tea extraction process.

The selected tea leaves are dried and ground into a fine powder. Subsequently, 25 grams of the powder are added to 500 mL of ethanol in the reactor system (Figure 1). The system is operated under controlled conditions of a stirring speed of 400 rpm and a temperature of 60 °C for 2 hours. The dark green solution is then centrifuged at 10000 rpm for 5 minutes to separate the powder from the solution. The resulting solution is then stored at 5 °C in a refrigerator.

### 2.2.2. The synthesis process of ZnO nanoparticles

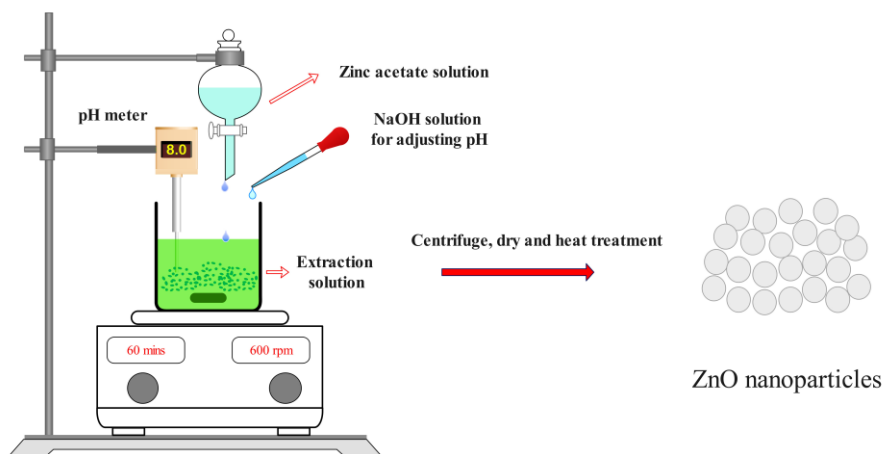


Figure 2. Synthesis process of ZnO nanoparticles

The synthesis of ZnO nanoparticles follows a similar approach to that described in our previous research [10]. 2 grams of  $\text{Zn}(\text{CH}_3\text{COO})_2 \cdot 2\text{H}_2\text{O}$  was dissolved in 20 mL of distilled water. The resulting solution was then dropwise into a 100 mL flask containing the prepared extraction solution. The entire solution was placed on a magnetic stirrer at a speed of 600 rpm and maintained at a pH of 8 using a 1 M NaOH solution. The stirring process was carried out for

60 minutes. After the reaction, the solution was centrifuged to collect the precipitate, which was dried overnight at 60 °C. Finally, the obtained powder was calcined at 600 °C for 3 hours.

### 2.2.3. The synthesis process of ZnO/PPy nanocomposites

0.1 grams of  $C_{14}H_{14}N_3NaO_3S$  were added to 60 mL of distilled water and stirred at room temperature. Then, 0.5 grams of  $FeCl_3$  were quickly added to the solution. Subsequently, 0.035 grams of ZnO nanoparticles were added, and the mixture was sonicated for an hour. A dark red solution was obtained, to which 0.362 mL of  $C_4H_5N$  were added and stirred for 24 hours. The resulting mixture was dried overnight at 60 °C.

### 2.2.4. Characterizations

The morphological properties of the materials were performed using a field emission scanning electron microscope (FESEM) S-4800, Hitachi, Japan, operating at a voltage of 3.0 kV under ambient conditions. The crystal structure characteristics of materials were obtained using the X-ray diffraction instrument, D8 Advance, BRUKER AXS, Germany with  $CuK\alpha$  radiation, 50 kV. The UV–vis spectra were recorded using Shimadzu UV-1800 Double Beam UV/Visible Scanning Spectrophotometer from Japan.

### 2.2.5. Gas sensing experiment

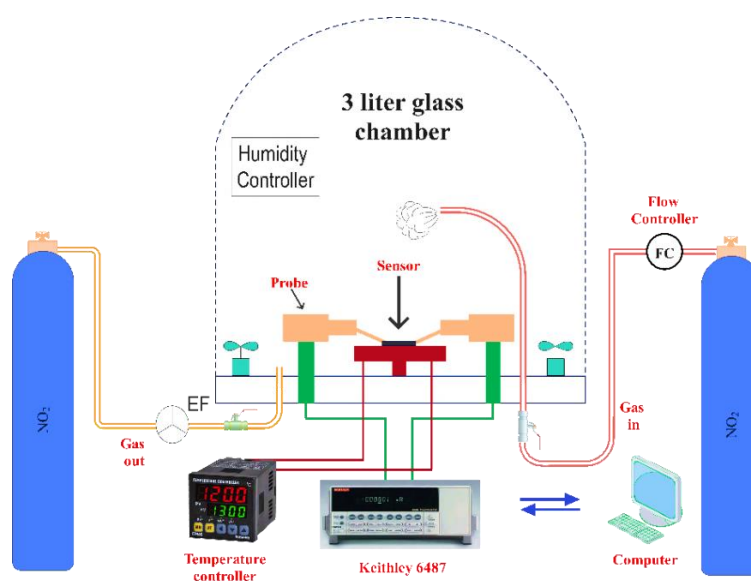


Figure 3. Schematic diagram of the gas sensing experiment.

The gas sensor was prepared by drop-casting a suspension of ZnO/PPy material in ethanol on an electrode, which was dried at 60 °C before conducting gas sensing experiments. The measurements were performed using a system connected to a computer and Keithley 6487 equipment at the School of Engineering Physics, Hanoi University of Science and Technology (Figure 3). The working temperature of the sensor is consistently maintained at 40 °C using a temperature controller. The control of humidity levels during the measurement process was achieved by humidity controller DQ 300 TRH 96.

The sensor response was quantified using the equation  $S = R_a/R_g$ , where  $R_a$  and  $R_g$  represent the resistances of the sensor in air and in the oxidizing gas NO<sub>2</sub>, respectively. The response time was determined as the duration required for the sensor to achieve 90 % of its saturation resistance after exposure to NO<sub>2</sub>. Similarly, the recovery time was defined as the duration needed for the sensor to return to 90 % of its initial resistance value after being exposed to air.

### 3. RESULTS AND DISCUSSION

#### 3.1. Materials characterization

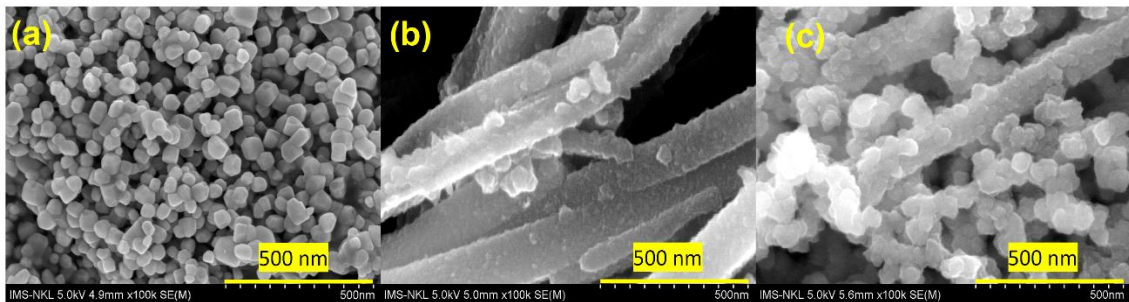


Figure 4. FESEM images of ZnO (a), PPy (b) and ZnO/PPy (c).

Figures 4a, b, and c depict the morphological characteristics of three distinct materials: ZnO, PPy, and the ZnO/PPy nanocomposite material, in a sequential manner. The ZnO nanoparticles in Fig 4a. display a relatively homogeneous size distribution spanning from 50 to 70 nm. On the other hand, the synthesized PPy material exhibits a rod-shaped structure, characterised by a diameter ranging from approximately 100 to 200 nm. Figure 4c demonstrates the ZnO/PPy nanocomposite system, consisting of PPy rods surrounded by ZnO particles.

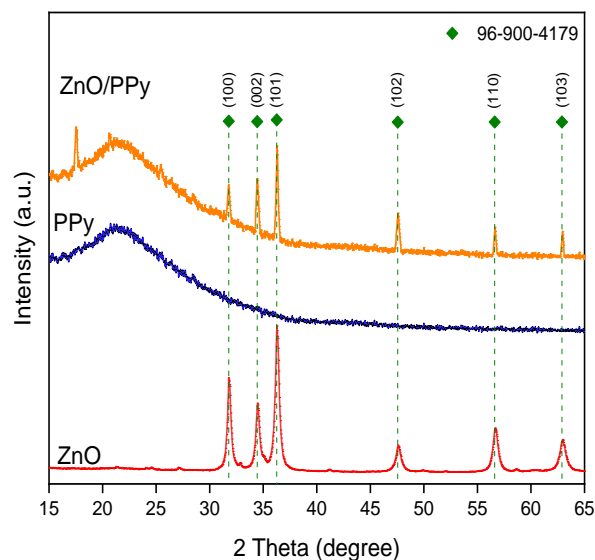


Figure 5. X-ray diffraction spectrum of materials.

The phase structures of ZnO, PPy, and ZnO/PPy materials are shown in Figure 5. Based on the intensity and characteristics of the peaks, the ZnO nanoparticles are evaluated to possess a high crystallinity while the phase of the Polypyrrole material was found to be amorphous [11]. The phase structure of the synthesized ZnO material exhibited a hexagonal shape, with characteristic peaks observed at positions corresponding to lattice planes (100), (002), (101), (102), (110), and (103) as referenced to the COD 96-900-4179. Additionally, the ZnO/PPy composite material displayed predominantly weaker peak signals than ZnO nanoparticles, which may be attributed to the low ZnO content in the composite. The signal at the broad peak at  $2\theta = 20.530^\circ$  of the composite also indicated the presence of Polypyrrole [12] while the strange peak at the position around  $17^\circ$  may be attributed to the formation of  $Zn(OH)_2$  during the reaction process without heat treatment [13].

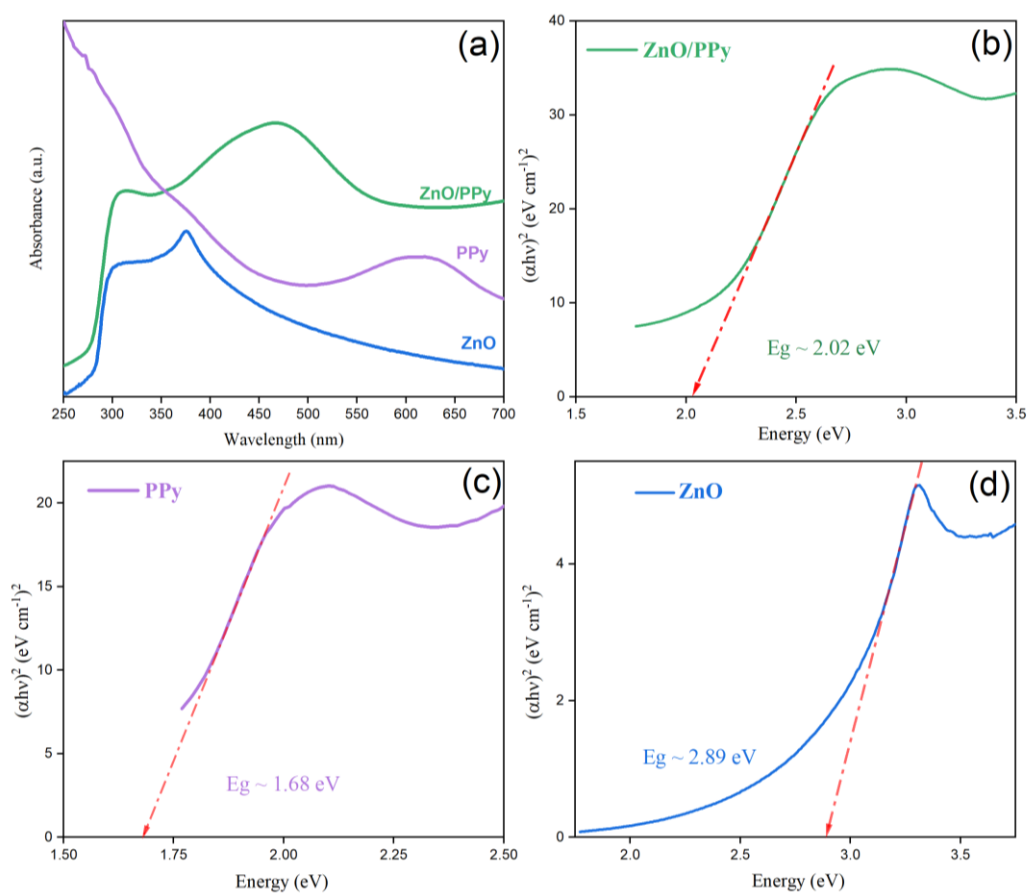


Figure 6. UV-Visible absorbance spectra of ZnO, ZnO/PPy, PPy (a) and band gap of ZnO/PPy nanocomposite (b), PPy (c) and ZnO (d).

Figure 6a. displays the UV-Vis spectra of ZnO NPs (blue line), PPy rods (violet line) and ZnO/PPy nanocomposites (green line). In consideration of these data, the energy band gap ( $E_g$ ) of three materials was calculated using the Tauc method [14]. The  $E_g$  of ZnO NPs is typically greater than 3.2 eV [15]; however, in this study, the  $E_g$  of ZnO NPs is approximately 2.89 eV (Figure 6d). According to Mansoob Khan et al., the reduction of the  $E_g$  is due to the modification of the surface with the functional groups from plant leaf extracts [16]. Additionally,

the estimated E<sub>g</sub> of the PPy rods and ZnO/PPy nanocomposites are approximately 1.68 eV and 2.02 eV, respectively (Fig 6 b, c). This result demonstrates a significant reduction in the E<sub>g</sub> of ZnO upon the modification with PPy, consistent with several previous publications [17, 18].

### 3.2. Gas sensing properties

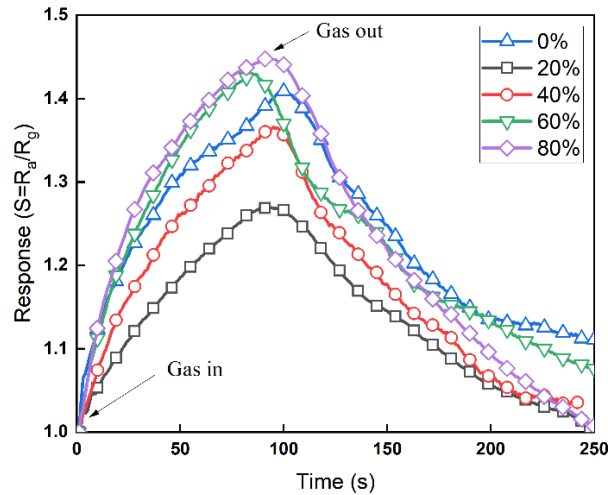


Figure 7. Relationship between sensitivity and humidity level.

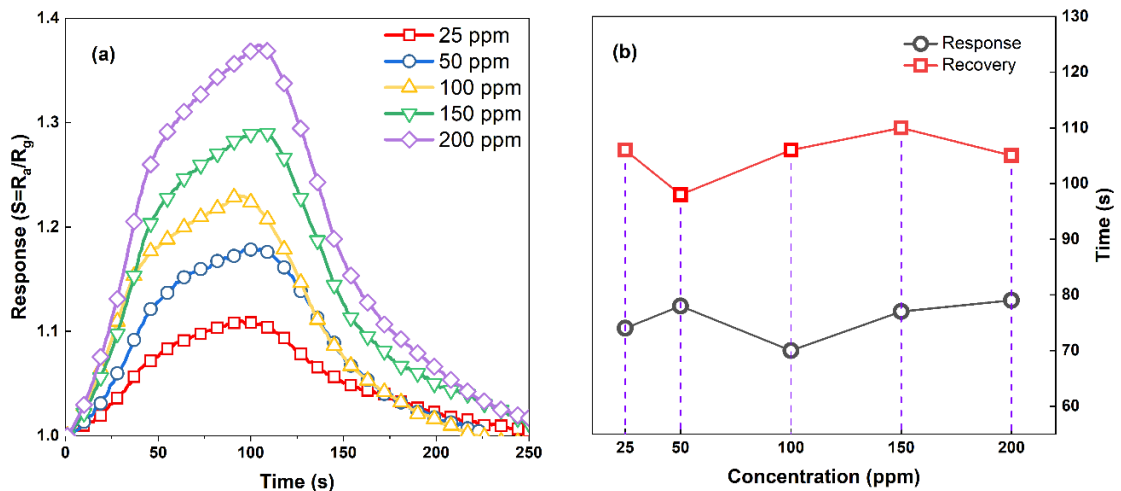


Figure 8. Gas response of ZnO/PPy (a) and sensor's response and recovery time (b) at different concentrations.

The impact of humidity on the gas sensitivity of the material is investigated at different humidity levels at 200 ppm NO<sub>2</sub> (Figure 7). When the humidity level is at 0 %, the numerical value of S is approximately 1.4089. When subjected to low humidity levels ranging from 20 % to 40 %, the observed values of S exhibited a significant decrease, reaching approximately 1.364 and 1.268. The observed decline can be attributed to the competitive adsorption phenomenon between NO<sub>2</sub> gas and water [19]. Conversely, under high humidity conditions, the magnitude of

S exhibited an increase in a low-moisture atmosphere, specifically reaching approximately 1.428 at a humidity level of 60 % and 1.447 at a humidity level of 80 %. It is hypothesized that under low-temperature conditions, the adsorption of many water molecules will occur on the surface of the composite material coated with predominantly ZnO nanoparticles. When the material interacts with NO<sub>2</sub> gas, the gas molecules will displace water molecules from the material's surface, resulting in a change in resistance and increased sensitivity [20].

After experimenting to assess the influence of humidity, the sensor was preserved in a vacuum environment for one day. Subsequently, the impact of NO<sub>2</sub> gas concentration was further investigated at 25, 50, 100, 150, and 200 ppm at 80% humidity (Figure 8a). In general, the sensor's sensitivity increases consistently as the concentration of NO<sub>2</sub> increases. Among them, the highest sensitivity values at 25, 50, 100, 150, and 200 ppm concentrations are 1.110, 1.179, 1.230, 1.292, and 1.374, respectively. Figure 8b illustrates that the sensor exhibits significantly faster response times than recovery times at each NO<sub>2</sub> concentration (approximately 20 to 30 seconds).

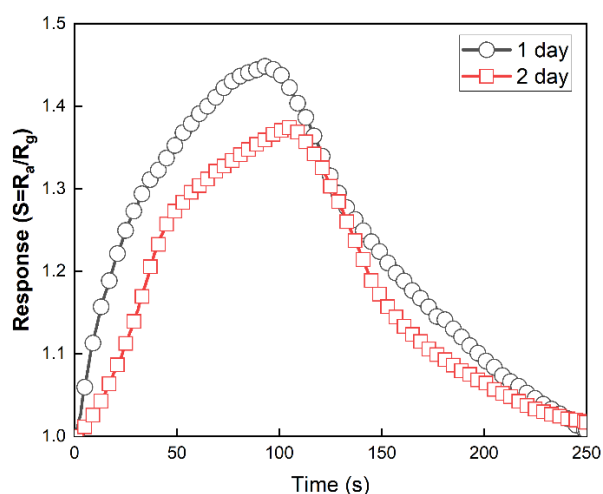


Figure 9. Assessment of sensor stability.

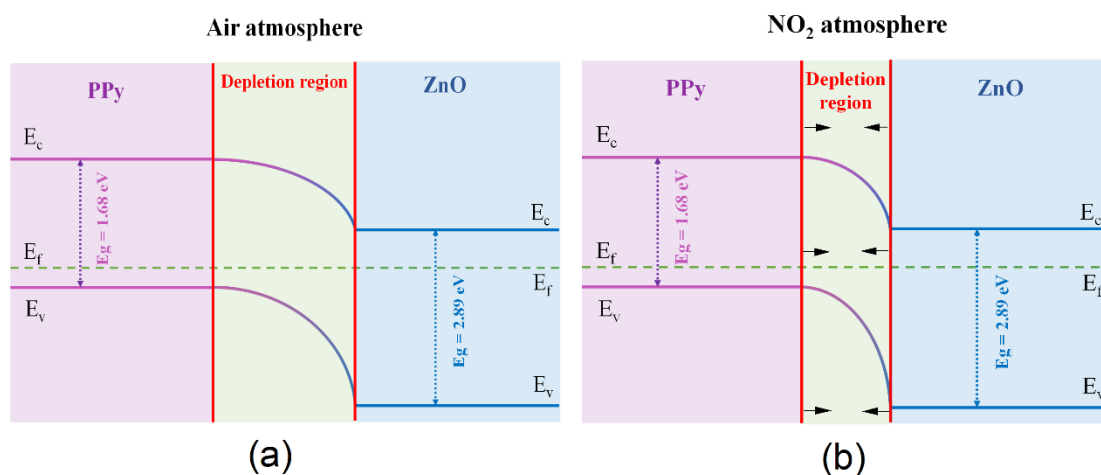


Figure 10. Schematic diagram of energy band for ZnO/PPy nanocomposites in the air atmosphere (a) and NO<sub>2</sub> atmosphere (b).



Additionally, the sensor's stability was assessed by our research team using information from the investigation of the impact of humidity and NO<sub>2</sub> concentration, as depicted in Figure 9. After one day, at a NO<sub>2</sub> concentration of 200 ppm and 80% humidity, the highest sensitivity of the sensor was decreased from 1.445 to 1.374. Moreover, some changes in the response and recovery times of the sensor were observed, albeit not significant.

The NO<sub>2</sub> gas-sensing mechanism of the nanocomposites can be explained based on schematic diagram illustrated in Fig. 10 (a-b). The Fermi energy level ( $E_f$ ) of Polypyrrole is situated near the valence band since it behaves as a p-type semiconductor [21]. In contrast, ZnO NPs is categorized as an n-type semiconductor [22], so its Fermi energy level is in close to the conduction band. The nanocomposites exhibit properties of p-n junction and the formation of the depletion region as shown in Fig 10a. It has been noted that the electrical resistance of the nanocomposites decreases upon exposure to oxidizing NO<sub>2</sub> gas. This suggests the p-type behavior, which also means that the predominant mode of charge transport occurs via PPy. Previous studies have affirmed that the interaction between NO<sub>2</sub> gas molecules and the  $\pi$ -electron networks of PPy leads to the reduction of resistance [23, 24]. Therefore, the width of the depletion region decreased (Fig 10b), facilitating the detection of small quantities of NO<sub>2</sub> gas molecules.

#### 4. CONCLUSIONS

ZnO nanoparticles were synthesized using a green approach, with green tea leaves employed as the reaction agent. The gas sensitivity of the nanocomposite material based on rod-like structure Polypyrrole with ZnO nanoparticles adhered onto its surface, was investigated at room temperature. The highest sensitivity value for 25 ppm NO<sub>2</sub> at a temperature of 40°C and 80% humidity is 1.109, while for 200 ppm NO<sub>2</sub> under similar conditions, the highest sensitivity value is 1.445. The response time ranged from 70 to 80 seconds, and the recovery time ranged from 100 to 110 seconds at different NO<sub>2</sub> concentrations. In general, ZnO/PPy is a promising material for NO<sub>2</sub> gas sensors; however, the stability, response time, and recovery time of the nanocomposites towards NO<sub>2</sub> also need to be improved in further studies.

**Acknowledgements.** This research is funded by the basic research grant from the Institute of Chemistry and Materials titled " Green synthesis of ZnO/conductive polymer for oriented application in the detection of toxic gases at defense production facilities" starting from March 2023.

**CRedit authorship contribution statement.** Vu Thanh Dong, Pham Tien Hung: Methodology, Investigation, Funding acquisition. Le Duc Anh, Dang Duy Khanh: Formal analysis. Ly Quoc Vuong, Nguyen Thi Huong: Formal analysis, Supervision.

**Declaration of competing interest.** The authors declare that they have no known competing financial interests or personal relationships that could have appeared to influence the work reported in this paper.

#### REFERENCES

1. Dhall S., B.R. Mehta, A.K. Tyagi, and K. Sood. - A review on environmental gas sensors: Materials and technologies. *Sens Int.*, **2** (2021): p. 100116. <https://doi.org/10.1016/j.sintl.2021.100116>
2. Li A. J., V. K. Pal, and K. Kannan. - A review of environmental occurrence, toxicity, biotransformation and biomonitoring of volatile organic compounds. *Environ Toxicol Chem.*, **3** (2021): p. 91-116. <https://doi.org/10.1016/j.enccco.2021.01.001>

3. Krishna K. G., S. Parne, N. Pothukanuri, V. Kathirvelu, S. Gandhi, and D. Joshi. - Nanostructured metal oxide semiconductor-based gas sensors: A comprehensive review. *Sens Actuators A Phys* **341** (2022): p. 113578. <https://doi.org/10.1016/j.sna.2022.113578>
4. Bhati V. S., M. Hojamberdiev, and M. Kumar. - Enhanced sensing performance of ZnO nanostructures-based gas sensors: A review. *Energy Rep.*, **6** (2020): p. 46-62. <https://doi.org/10.1016/j.egy.2019.08.070>
5. Zhang B., M. Li, Z. Song, H. Kan, H. Yu, Q. Liu, G. Zhang, and H. Liu. - Sensitive H<sub>2</sub>S gas sensors employing colloidal zinc oxide quantum dots. *Sens Actuators B Chem*, **249** (2017): p. 558-563. <https://doi.org/10.1016/j.snb.2017.03.098>
6. Kang Y., F. Yu, L. Zhang, W. Wang, L. Chen, and Y. Li. - Review of ZnO-based nanomaterials in gas sensors. *Solid State Ionics*, **360** (2021): p. 115544. <https://doi.org/10.1016/j.ssi.2020.115544>
7. Franco M. A., P. P. Conti, R. S. Andre, and D. S. Correa. - A review on chemiresistive ZnO gas sensors. *Sens. Actuators Rep.*, **4** (2022): p. 100100. <https://doi.org/10.1016/j.snr.2022.100100>
8. Zhang, C., Y. Luo, J. Xu, and M. Debliqy. - Room temperature conductive type metal oxide semiconductor gas sensors for NO<sub>2</sub> detection. *Sens Actuators A Phys*, **289** (2019): p. 118-133. <https://doi.org/10.1016/j.sna.2019.02.027>
9. Harpale, K., P. Kolhe, P. Bankar, R. Khare, S. Patil, N. Maiti, M.G. Chaskar, M.A. More, and K.M. Sonawane. - Multifunctional characteristics of polypyrrole-zinc oxide (PPy-ZnO) nanocomposite: Field emission investigations and gas sensing application. *Synth. Met.*, **269** (2020): p. 116542. <https://doi.org/10.1016/j.synthmet.2020.116542>
10. Pham, T.M.H., M.T. Vu, T.D. Cong, N.S. Nguyen, T.A. Doan, T.T. Truong, and T.H. Nguyen. - Green sonochemical process for preparation of polyethylene glycol-Fe<sub>3</sub>O<sub>4</sub>/ZnO magnetic nanocomposite using rambutan peel extract as photocatalyst, for removal of methylene blue in solution. *Bull. Mater. Sci.*, **45** (1) (2022): p. 13. <https://doi.org/10.1007/s12034-021-02584-2>
11. Pirsá, S., T. Shamusí, and E.M. Kia. - Smart films based on bacterial cellulose nanofibers modified by conductive polypyrrole and zinc oxide nanoparticles. *J. Appl. Polym. Sci.*, **135** (34) (2018): p. 46617. <https://doi.org/10.1002/app.46617>
12. Shrikrushna, S., J.A. Kher, M.V.J.J.o.N. Kulkarni, and Nanotechnology. - Influence of dodecylbenzene sulfonic acid doping on structural, morphological, electrical and optical properties on polypyrrole/3C-SiC nanocomposites. *J. Nanomed. Nanotechnol.*, **6** (5) (2015): p. 1. <https://doi.org/10.4172/2157-7439.1000313>
13. Hussain, A., Shumaila, A. Dhillon, I. Sulania, and A.M. Siddiqui. - Comparative Study of Polypyrrole/Zinc Oxide Nanocomposites Synthesized by Different Methods. in *Proceedings of the International Conference on Atomic, Molecular, Optical & Nano Physics with Applications*. Singapore 2022. pp. 601-607
14. Haryński, Ł., A. Olejnik, K. Grochowska, and K. Siuzdak. - A facile method for Tauc exponent and corresponding electronic transitions determination in semiconductors directly from UV-Vis spectroscopy data. *Opt. Mater.*, **127** (2022): p. 112205. <https://doi.org/10.1016/j.optmat.2022.112205>

15. Hjiri, M., F. Bahanan, M.S. Aida, L. El Mir, and G. Neri. - High Performance CO Gas Sensor Based on ZnO Nanoparticles. *J. Inorg. Organomet. Polym. Mater.*, **30** (10) (2020): p. 4063-4071. <https://doi.org/10.1007/s10904-020-01553-2>
16. Khan, M.M., N.H. Saadah, M.E. Khan, M.H. Harunsani, A.L. Tan, and M.H. Cho. - Potentials of *Costus woodsonii* leaf extract in producing narrow band gap ZnO nanoparticles. *Mater. Sci. Semicond. Process.*, **91** (2019): p. 194-200. <https://doi.org/10.1016/j.mssp.2018.11.030>
17. Chougule, M.A., S. Sen, and V.B. Patil. - Polypyrrole–ZnO hybrid sensor: Effect of camphor sulfonic acid doping on physical and gas sensing properties. *Synth. Met.*, **162** (17) (2012): p. 1598-1603. <https://doi.org/10.1016/j.synthmet.2012.07.002>
18. Balakumar, V. and A. Baishnisha. - Rapid visible light photocatalytic reduction of Cr<sup>6+</sup> in aqueous environment using ZnO-PPy nanocomposite synthesized through ultrasonic assisted method. *Surf. Interfaces*, **23** (2021): p. 100958. <https://doi.org/10.1016/j.surfin.2021.100958>
19. Duoc, V.T., C.M. Hung, H. Nguyen, N.V. Duy, N.V. Hieu, and N.D. Hoa. - Room temperature highly toxic NO<sub>2</sub> gas sensors based on rootstock/scion nanowires of SnO<sub>2</sub>/ZnO, ZnO/SnO<sub>2</sub>, SnO<sub>2</sub>/SnO<sub>2</sub> and, ZnO/ZnO. *Sens Actuators B Chem*, **348** (2021): p. 130652. <https://doi.org/10.1016/j.snb.2021.130652>
20. Liu, B., X. Liu, Z. Yuan, Y. Jiang, Y. Su, J. Ma, and H. Tai. - A flexible NO<sub>2</sub> gas sensor based on polypyrrole/nitrogen-doped multiwall carbon nanotube operating at room temperature. *Sens Actuators B Chem*, **295** (2019): p. 86-92. <https://doi.org/10.1016/j.snb.2019.05.065>
21. Das, M. and S. Roy. - Polypyrrole and associated hybrid nanocomposites as chemiresistive gas sensors: A comprehensive review. *Mater. Sci. Semicond. Process.*, **121** (2021): p. 105332. <https://doi.org/10.1016/j.mssp.2020.105332>
22. Li, G., Z. Sun, D. Zhang, Q. Xu, L. Meng, and Y. Qin. - Mechanism of Sensitivity Enhancement of a ZnO Nanofilm Gas Sensor by UV Light Illumination. *ACS Sensors*, **4** (6) (2019): p. 1577-1585. <https://doi.org/10.1021/acssensors.9b00259>
23. Mane, A.T., S.T. Navale, S. Sen, D.K. Aswal, S.K. Gupta, and V.B. Patil. - Nitrogen dioxide (NO<sub>2</sub>) sensing performance of p-polypyrrole/n-tungsten oxide hybrid nanocomposites at room temperature. *Org. Electron.*, **16** (2015): p. 195-204. <https://doi.org/10.1016/j.orgel.2014.10.045>
24. Nellaiappan, S., K.S. Shalini Devi, S. Selvaraj, U.M. Krishnan, and J.V. Yakhmi. - Chemical, Gas and Optical Sensors Based on Conducting Polymers, in *Advances in Hybrid Conducting Polymer Technology*, S. Shahabuddin, et al., Editors, Springer International Publishing: Cham. 2021, p. 159-200.